Available online at www.sciencedirect.com
SCIENCE DIRECT
Surface & Coatings Technology 200 (2006) 3486 – 3491
SURFACE & COATINGS TECHNOLOGY
www.elsevier.com/locate/surfcoat

Sol-gel coatings on carbon steel: Electrochemical evaluation

Andrés Pepe [a], Pablo Galliano [a], Mario Aparicio [b], Alicia Durán [b], Silvia Ceré [a,*]

[a] INTEMA, Division Corrosion, Universidad Nacional del Mar del Plata, Juan B. Justo 4302.B7608FDQ, Mar del Plata, Argentina
[b] Instituto de Cerámica y Vidrio (CSIC), Campus de Cantoblanco, 28049 Madrid, Spain

Received 9 August 2004; accepted in revised form 28 July 2005
Available online 19 September 2005

Abstract

Degradation of carbon steel has always been a concern. The use of coatings is especially recommended in aggressive atmospheres at moderate temperatures. Ceramic films can be used to improve the resistance against high temperature oxidation and corrosion of metals. Amid the different options, a sol-gel process provides a low cost, simple and non-hazardous method for processing ceramic coating with controllable composition and microstructure.

This work evaluates the electrochemical behaviour of carbon steel coated by sol-gel method. Hybrid organic–inorganic silica sol-gel coatings were obtained by dip coating of planar samples in an organically modified silica sol made from hydrolysis and polycondensation of tetra-orthosilicate (TEOS) and methyltriethoxisilane (MTES) by acidic catalysis. Coatings free of defects were obtained at a sintering temperature of 400 °C. The coated samples were inspected by optical and electron microscopy and coating thickness was measured by using a Talystep surface roughness tester. Electrochemical evaluation was made by electrochemical impedance spectroscopy (EIS) and potentiodynamic polarization curves. A comparison of the corrosion resistance of the coated metal with the uncoated one is presented. The measurements show the improvement of the corrosion resistance of the coated carbon steel.

Keywords: Impedance spectroscopy; Sol-gel; Iron alloy

1. Introduction

The protection of metals against environmental attack is usually achieved by using to an adherent and protective coating deposited onto the metal surface. The fabrication of coating films starting from metal alkoxides is a promising application of sol-gel techniques.

The advantages and technological significance of the sol-gel method have been demonstrated [1,2] being an attractive way to implement corrosion and oxidation protection [3–5]. The interest for sol-gel coatings is focused on hybrid organic-inorganic coatings in order to get higher critical thickness than with inorganic ones. Hybrid systems are obtained from the structural incorporation of organic groups, such as methyltriethoxisilane (MTES) in the precursor solutions, thus incorporating organic groups in SiO_2 coatings. Sintering temperatures higher than 550 °C lead to mostly inorganic coatings, due to oxidation of CH_3 [6].

Several coatings produced by sol-gel processing have been studied extensively for prevention of corrosion in stainless steel and other metals that naturally form a passive layer on their surface [7], although sol-gel deposition on active corroding materials such as iron remains unexplored.

This work evaluates the electrochemical behaviour of carbon steel coated by a sol-gel method. Hybrid organic–inorganic silica sol-gel coatings were obtained by dip coating of planar samples in an organically modified silica sol made from the hydrolysis and polycondensation of tetra-orthosilicate (TEOS) and methyltriethoxisilane (MTES). The coating structure is formed by a silica network of Si–O–Si bonds interrupted in some points by CH_3 groups attached to silicon atom from MTES. Electrochemical

* Corresponding author. Tel.: +54 223 4816600; fax: +54 223 4810046.
E-mail address: smcere@fi.mdp.edu.ar (S. Ceré).

0257-8972/$ - see front matter © 2005 Elsevier B.V. All rights reserved.
doi:10.1016/j.surfcoat.2005.07.102

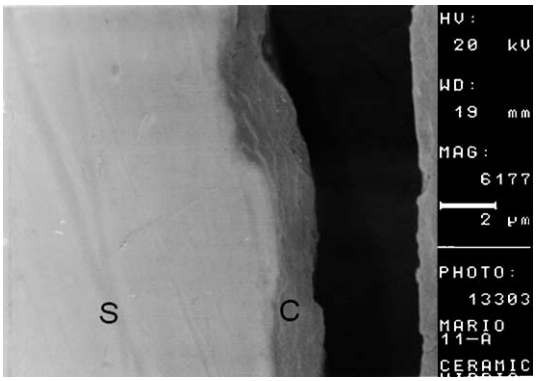

Fig. 1. SEM photograph of a transverse section of the coated carbon steel. In the photograph, "C" indicates the coating and "S" the substrate.

evaluation of the coatings and their comparison with the bare material are presented.

2. Experimental

2.1. Substrates

Coatings were made on 8 cm^2 carbon steel sheets (AISI 1005) and sodium lime glass samples 12 cm^2 in size. All samples were hand washed with acetone and then ultrasonically cleaned for 30 min in isopropylic alcohol.

2.2. Sol synthesis

Hybrid organic–inorganic silica sol was made from hydrolysis and polycondensation of tetra-orthosilicate (TEOS) and methyltriethoxisilane (MTES) in a molar ratio of 40:60 in an acidic catalysis using ethanol as the solvent. The synthesis was made under reflux during a 4-h period. The detailed preparation process is described elsewhere [8]. After the process, the pH was modified to a value of 5±0.5 by the addition of filtered 5.0 N NaOH prepared in an ethanol solution.

2.3. Coating procedure

Hybrid organic–inorganic silica coatings were made by sample immersion in freshly prepared sol followed by withdrawal at a constant velocity of 28 cm min^{-1}. After exposure for 30 min at room temperature, samples were treated at 400 °C for 15 min in an electric oven with an air atmosphere. This procedure was done twice in order to get thicker coatings.

2.4. Coating characterisation

Coated samples were inspected by optical and electron microscopy (Olympus PMG3 and Philips SEM 505, respectively). Coating surface roughness was measured by a roughness tester (Surtronic 3+) with a vertical resolution of 10 nm and horizontal resolution less than 8 nm. Coating thickness was measured on glass samples after densification by means of a profilometer (Talystep, Taylor-Hobson, UK) on a scratch made immediately after deposition. The coating thickness was stated as the average of at least five independent measurements on each sample.

2.5. Electrochemical assays

Electrochemical assays were conducted in a conventional three electrode cell in aerated 3.5 wt.% NaCl solution prepared from p.a. grade chemicals (Aldrich) and bidistilled water (Millipore). A saturated calomel electrode (SCE, Radiometer Copenhagen, +0.24 V vs. NHE) was employed as the reference electrode and a platinum wire of convenient area as counter electrode. Electrochemical impedance spectroscopy (EIS) was performed sweeping frequencies from 20 000 to 0.01 Hz and modulating 0.010 V (rms) around the corrosion potential (E_{corr}). Potentiodynamic polarization curves were recorded from the corrosion potential to 0.9 V at 0.002 V s^{-1}. Polarization resistance measurements were recorded by sweeping ±0.010 V around a corrosion potential at 0.002 V s^{-1}. Assays were achieved in an electrochemical unit (Solartron 1280B and Voltalab PGP201). EIS fitting was performed using a *Z* plot software [9].

3. Results and discussion

Fig. 1 shows an SEM photograph of a transverse section of an unpolished coated carbon steel. It can be observed that the coating is well bonded and is free of defects such as surface blistering or cracks. The coating thickness measured on glass samples was 1.14±0.05 µm. Roughness assays on

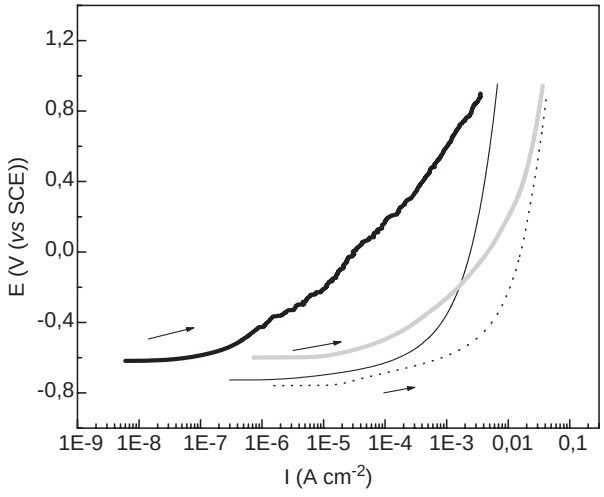

Fig. 2. Polarization curves for the bare and coated material after 2 and 48 hours of immersion in aerated 3.5% NaCl. $v = 0.002$ V s^{-1}. (Bare steel: — 2 h immersion; ··· 48 h immersion. Coated steel: ■ 2 h immersion, ▬ 48 h immersion.)

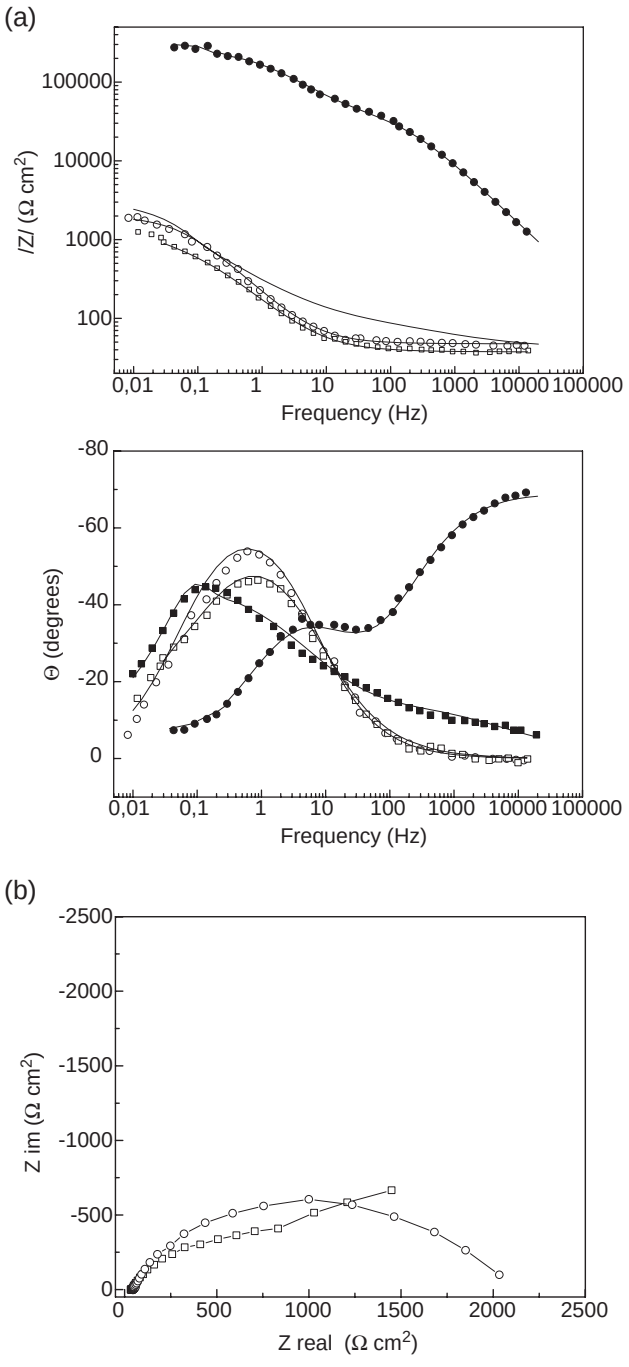

Fig. 3. (a) EIS Bode plots spectra for the bare and coated materials after 2 and 48 h of immersion: (⋆) coated steel 2 h immersion; (■) coated steel 48 h immersion; (>) bare steel 2 h immersion; (□) bare steel 48 h immersion. Solid lines represent modelled results. (b) EIS Nyquist plot for the bare material after 2 and 48 h of immersion: (>) bare steel 2 h immersion; (□) bare steel 48 h immersion.

bare steel presented an average roughness (*Ra*) of 0.88 μm while for coated steel *Ra* diminishes to 0.61 μm.

With the aim of comparing corrosion susceptibility of the coated system in relation to the uncoated metal, anodic polarization curves of both materials were recorded. Fig. 2 shows polarization curves of the bare and coated material after 2 and 48 h of immersion in aerated NaCl. The bare steel shows active dissolution, while the coated material shows a pathway of lower current densities than the bare material. This is an indication that the coating is inhibiting the anodic process, acting as a barrier to the electrolyte by impeding its contact with the metal surface.

EIS diagrams in the Bode format are presented in Fig. 3a. Bare material after 2 h of immersion shows one time constant, and after 48 h of immersion the spectrum shows a change in the Bode Phase plot (Theta vs. freq.) spectrum suggesting that the system's response can be composed of two different contributions: the one at higher frequencies could be associated with the oxide response resulting from penetration of the electrolyte through a porous film on the base material; the second one at low frequencies could be related to the metal response [10]. Fig. 3b shows the same data presented in Fig. 3a for the bare material in the Nyquist form, where the two time constant for the uncoated material after 48 h of immersion are more clearly observed. The electrochemical behaviour can be described in terms of an equivalent circuit in order to provide the most relevant parameters applicable to the corroding system. A constant phase element (CPE) was used instead an "ideal" capacitor, taking into account that the slopes of the curves in the log /*Z*/ vs. log f plot were not −1 (value expected for and ideal capacitor) and certain degree of inhomogeneity in the surface.

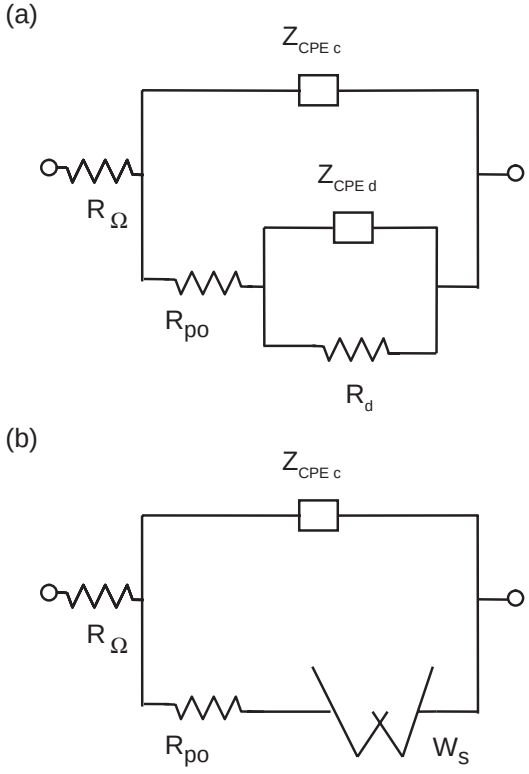

Fig. 4. Equivalent circuits used for data fitting for: a) bare metal after 48 h immersion, coated metal after 2 h immersion; b) coated metal after 48 h of immersion.

Table 1
Parameters obtained from data fitting of bare steel after 2 and 48 h of immersion, and coated steel after 2 h of immersion (Fig. 3) with the equivalent circuit shown in Fig. 4a

	R_Ω (Ω cm^2)	Y_{0c} (Ω^{-1} cm^{-2} s^n)	n_c	R_{p0} (Ω cm^2)	Y_{0d} (Ω^{-1} cm^{-2} s^n)	n_d	R_t (Ω cm^2)
Bare mild steel 2 h immersion	23.1±0.71				$1.16\times10^{-3}\pm3.0\times10^{-5}$	0.78±0.01	$1.68\times10^{3}\pm7.1\times10^{2}$
Bare mild steel 48 h immersion	19.64±0.11	$1.27\times10^{-3}\pm1.75\times10^{-5}$	0.78±0.004	$1.1\times10^{3}\pm28.1$	$1.11\times10^{-2}\pm1.3\times10^{-3}$	0.95±0.05	$1.72\times10^{3}\pm2.06\times10^{2}$
Coated mild steel 2 h immersion	21.3±3.4	$1.13\times10^{-7}\pm5.43\times10^{-9}$	0.78±0.004	$4.3\times10^{4}\pm1.5\times10^{3}$	$1.14\times10^{-6}\pm5.47\times10^{-8}$	0.68±0.01	$2.23\times10^{5}\pm6.5\times10^{3}$

A CPE impedance is described by the expression:

$$Z_{CPE}=\frac{1}{Y_0(j\omega)^n}\quad -1\le n\le 1\quad [11] \tag{1}$$

where n is a coefficient associated to the system homogeneity (being 1 for an ideal capacitor), ω is the frequency and Y_0 is the pseudocapacitance of the system. Y_0 can be represented by:

$$Y_0=\frac{r\varepsilon\varepsilon_0 A}{d} \tag{2}$$

where ε_0 is the permittivity of free space, ε is the dielectric constant of the surface film, d is the film thickness, A is the exposed area and r is the roughness factor [12]. Fig. 4a shows the equivalent circuit used to model the uncoated system after 48 h of immersion where R_Ω represents the electrolyte resistance, CPE_c is related with the non ideal capacitance of the oxide film, R_{po} is the resistance presented by the oxide film to the passage of the electrolyte, CPE_d is related to the non-ideal capacitance of the double layer of the bare metal and R_d is the charge transfer resistance. The bare material after 2 h of immersion can be modelled by a simple circuit with CPE_d lying in parallel with the double layer resistance, R_d. The main parameters obtained from fitting data are shown in Table 1. The evolution of EIS spectra with time for the bare material can be observed in Fig. 3a and b and its fitted data is listed in Table 1.

Fig. 3a also shows the spectra for the coated samples. It can be seen that after 2 h of immersion two maxima in the Bode plot Theta vs. freq. can be observed. Substrate degradation can proceed through pore and/or defects. This process could be under charge transfer control because there is no evidence of diffusion control related to any movement restrictions between the solution and the metal or its superficial oxide. The equivalent circuit used represents the electrochemical behaviour of a metal covered with an unsealed porous film (Fig. 4a) and the values obtained form the circuit modelling are presented in Table 1. As the pseudocapacitance value is too high to be related to a non-conductive coating, it is possible to assume that the time constant associated with the coating would be located at higher frequencies and would not be in the spectrum due to limitations of the equipment. The two time constants that are observed in the coated spectrum would correspond to the attack occurring in the metallic substrate and in the oxide formed at the base of the pores, thus explaining why both pseudocapacitances (Y_0) reach values with a similar order of magnitude [13].

After 48 h of immersion, the system's response changes with respect to the initial state. However, the presence of a change in the slope in the higher and lower frequency range still reflects the existence of two time constants. The shape of the spectra suggests that the dielectric properties of the coating may be affected due to the immersion process and the phase angle shift indicates a less capacitive response probably due to solution permeation through the coating causing localised corrosion [10]. The impedance data shown in Fig. 3 for the double layer coating after 48 h of immersion present a Warburg behaviour in the spectra that could be attributed to a diffusion process taking place in the solid phase. The Warburg impedance and the CPE with an n value around 0.5 (the latter known as "infinite diffusion") are used to model increasing ionic conductivity due to corrosion processes occurring inside the pores and the increasing diffusivity into them. If the material is thin, low frequencies will penetrate the entire thickness, creating a finite length Warburg element. Only if the material is thick enough so that the lowest frequencies do not penetrate the layer, it can be interpreted as infinite (Eq. (3)) [9].

$$Z_w=\frac{R_{DO}}{(jT\omega)^n}\tanh(jT\omega)^n \tag{3}$$

where R_{DO} is associated with solid phase diffusion and T is related to diffusion coefficient and pore length. Fig. 4b shows the equivalent circuit used for the data fitting. The phase angle decreases at low frequencies without reaching a zero value, suggesting the presence of pores in the outer part of the coating and diffusion effects inside [14].

Table 2
Parameters obtained from data fitting of coated steel after 48 h of immersion (Fig. 3) with the equivalent circuit shown in Fig. 4b

	R_Ω (Ω cm^2)	Y_{0c} (Ω^{-1} cm^{-2} s^n)	n_c	R_{p0} (Ω cm^2)	R_{DO} (Ω cm^2)	n_d	T
Coated mild steel 48 h immersion	28.2±2.17	$6.2\times10^{-4}\pm7.35\times10^{-5}$	0.449±0.0144	244±19.3	$1.63\times10^{4}\pm1.5\times10^{3}$	0.68±0.01	8.68±0.45

Table 3
Comparison between R_p data from direct current experiments and EIS data (from Tables 1 and 2)

	R_p (Ω cm^2)	R_p (EIS) (Ω cm^2)	E_{corr} (V)
Bare mild steel 2 h immersion	$4.71\times10^3\pm3.60\times10^2$	1.68×10^3	-0.736 ± 0.01
Bare mild steel 48 h immersion	$2.63\times10^3\pm1.25\times10^2$	2.83×10^3	$-0.757\pm5\times10^{-3}$
Coated mild steel 2 h immersion	$1.13\times10^5\pm6.5\times10^{-3}$	2.63×10^5	$-0.588\pm9.2\times10^{-3}$
Coated mild steel 48 h immersion	$1.18\times10^4\pm1.47\times10^3$	1.64×10^4	$-0.610\pm6.6\times10^{-3}$

Fitting analysis showed that the pseudocapacitance regarding the coating interface changes its value by three orders of magnitude, while the resistance drastically decreases with respect to the initial immersion time (Tables 1 and 2). The increasing values of pseudocapacitance could be associated with an increase in the exposed area of the metal and electrolyte penetration in the coating through the breaks and pores that increase with time. On the other hand, the reduction of the R_{po} values can be related to an increase in pore area offering a low resistance to the electron transfer in the base of the pores. R_{DO}, which is associated with the diffusion resistance in the solid phase, presents a relatively high value probably due to the porous characteristics of the ferric oxide formed in the rupture.

Linear potential resistance (R_p) measurements were conducted in order to compare these values with the ones measured by EIS. As can be observed in Table 3, the tendency of the obtained values is maintained and this is especially useful for quick coating evaluation in field measurements where EIS facilities are not available.

Porosity (P) can be estimated by the following equation [15].

$$P = \frac{R_{ps}}{R_p} \times 10^{-\left|\frac{\Delta E_{corr}}{b_a}\right|} \times 100 \quad (4)$$

where R_p is the polarization resistance of the coating, R_{ps} is the polarization resistance of the bare steel, b_a is the Tafel slope of the bare steel and ΔE_{corr} is the difference in corrosion potential between the coated and bare substrate. The Tafel slope was determined from the data of Fig. 2 and a value of 0.126 V dec^{-1} was obtained. R_{ps} and R_p data can be obtained from Table 3. Porosity values calculated according to Eq. (4) are presented in Table 4. Porosity values suggest that the film is acting as a good barrier to electrolyte with a very low porosity during the first stages of soaking which is in good agreement with the microscopic observation of the coating shown in Fig. 1. The coating deposited on the metal substrate has a residual porosity after the annealing treatment even when they were not exposed to the aggressive electrolyte. Those pores are of nanometric in size and they are not interconnected. It has been previously demonstrated [6] that the same kind of coating that the one presented in this work, but applied on AISI 316L, improves the corrosion resistance of the substrate, suggesting that there is no pore interconnection. The two-layer mechanism of deposition as well as the hybrid structure of the film contributes to reduce porosity in the coating as already demonstrated by other authors [16,17]. After 48 h of soaking, localised corrosion occurring in the pores propagates under the surface film, creating a more voluminous oxide that finally delaminates the coating. This fact was checked by optic microscopy.

Table 4
Average porosity of sol-gel coating after 2 and 48 h of immersion

	% P
Coated mild steel 2 h immersion	0.278
Coated mild steel 48 h immersion	7.73

4. Conclusions

Continuous and crack free hybrid organic–inorganic silica coatings were obtained onto a corrodible surface such as carbon steel by the sol-gel route. Although coatings are an effective barrier against corrosive environment in the first stages of immersion, this protection seems to be reduced due to the propagation of localised corrosion underneath the surface film after 48 h of testing.

A good correlation between R_p measured by direct current techniques and R_p values obtained by EIS technique was found, which is a useful tool for field evaluation of coatings.

Acknowledgements

The authors would like to thank CYTED, project VIII-9 and TWAS Research Grant (RG/CHE/LA 01-216-217) for their support.

References

[1] C.J. Brinker, G.W. Scherer, Sol Gel Science. The Physics and Chemistry of Sol-Gel Processing, Academic Press, San Diego, 1990, p. 881.
[2] J. Zarzycki, J. Sol-Gel Sci. Technol. 8 (1997) 17.
[3] M. Guglielmi, J. Sol-Gel Sci. Technol. 8 (1997) 443.
[4] O. De Sanctis, L. Gómez, A. Marajofsky, C. Parodi, N. Pellegri, A. Durán, J. Non-Cryst. Solids 121 (1990) 338.
[5] P. Innocenzi, M. Guglielmi, M. Gobbin, P. Colombo, J. Eur. Ceram. Soc. 10 (1992) 431.
[6] J. Gallardo, I. García, M.A. Arenas, A. Conde, A. Durán, J. Sol-Gel Sci. Technol. 27 (2003) 175.
[7] T.P. Chou, C. Chandrasekaran, S.J. Limmer, S. Seraji, Y. Wu, M.J. Forbess, C. Nguyen, G.Z. Cao, J. Non-Cryst. Solids 290 (2001) 153.

[8] J. Gallardo, P. Galliano, A. Durán, J. Sol-Gel Sci. Technol. 19 (2000) 393.
[9] *Z* Plot for Windows, Electrochemical Impedance Software Operating Manual: Part I, Scribner Associates, Inc., Southern Pines, NC, 1998.
[10] C. Liu, Q. Bi, A. Leyland, A. Matthews, Corros. Sci. 45 (2003) 1243.
[11] CMS100 Sytems, Operator's Manual Addendum. Changes for CE Compliance, Gamry Instruments, Inc., Pennsylvani, USA, 1996.
[12] C. Liu, Q. Bi, A. Leyland, A. Matthews, Corros. Sci. 45 (2003) 1257.
[13] A. Conde, J.J. Damborenea, Corros. Sci. 44 (2002) 1555.
[14] M. Metikos-Hukovic, E. Tkalcec, A. Kwokal, J. Piljac, Surf. Coat. Technol. 165 (2003) 40.
[15] J. Creus, H. Mazille, H. Idrissi, Surf. Coat. Technol. 130 (2000) 224.
[16] J. Gallardo, P. Galliano, A. Durán, J. Sol-Gel Sci. Technol. 19 (2000) 107.
[17] J. Gallardo, A. Durán, D. di Martino, R. Almeida, J. Non-Cryst. Solids 298 (2002) 219.